Arch. Mech., 32, 5, pp. 663–674, Warszawa 1980

Navier-Stokes analysis of the pumping plate flow field

B. GAMPERT and T. ABDELHAFEZ (ESSEN)

THE FLOW field past a pumping plate is investigated for the case when the plate is moving with the velocity u_w in a fluid initially at rest and for cases when the velocity of the free stream is different from zero. First similarity solutions of the boundary layer equation are given. Then for various u_∞- and u_w- values the full time-dependent Navier-Stokes equations are integrated numerically by applying an explicit finite difference scheme. Differences between Navier-Stokes and boundary-layer-theory local skin friction results become smaller with increasing x-values and, about one third of the plate length away from the leading edge, the difference approaches zero. Largest differences are of about 15%. The Navier-Stokes analysis confirms the result obtained from the boundary layer theory which states that for $|u_\infty - u_w|$ fixed, the skin friction coefficient is larger for $u_w > u_\infty$ than for $u_w < u_\infty$. The difference between the two c_f-values reduces for smaller values of $|u_\infty - u_w|$ being of about 30% for $|u_\infty - u_w| = 1$ and being smaller than 1% for $|u_\infty - u_w| = 0.1$.

Rozważa się pole przepływu wokół płyty napędzającej w przypadku, gdy płyta porusza się z prędkością u_w w płynie o zerowej prędkości początkowej oraz w przypadkach, gdy prędkość strumienia swobodnego jest różna od zera. Podano pierwsze rozwiązania podobieństwa dla równania warstwy przyściennej. Następnie scałkowano numerycznie pełne (zawierające człon czasowy) równania Naviera-Stokesa posługując się schematem różnic skończonych. Różnice w tarciu powierzchniowym obliczanym z równań Naviera-Stokesa oraz z teorii warstwy przyściennej zmniejszają się przy wzroście wartości x i w okolicy jednej trzeciej długości płyty (licząc od krawędzi natarcia) różnice te zmierzają do zera. Największe różnice sięgają 15%. Analiza oparta na równaniach Naviera-Stokesa potwierdza wnioski otrzymane z teorii warstwy przyściennej stwierdzające, że przy ustalonym $|u_\infty - u_w|$ współczynnik tarcia powierzchniowego jest większy dla $u_w > u_\infty$ niż dla $u_w < u_\infty$. Różnica między wartościami c_f zmniejsza się przy malejących wartościach $|u_\infty - u_w|$ i wynosi około 30% dla $|u_\infty - u_w| = 1$ oraz poniżej 1% dla $|u_\infty - u_w| = 0{,}1$.

Рассматривается поле течения вокруг приводящей плиты, когда плита движется со скоростью u_w в жидкости с нулевой начальной скоростью, а также в случаях, когда скорость свободного потока отлична от нуля. Приведены первые решения подобия для уравнения пограничного слоя. Затем проинтегрированы численно полные (содержавшие временной член) уравнения Навье-Стокса, послуживаясь схемой конечных разностей. Разницы в поверхностном трении, расчитанным из уравнений Навье-Стокса, а также из теории пограничного слоя, уменьшаются при росте значения x, а в окрестности 1/3 длины плиты (считая от грани атаки) эти разницы стремятся к нулю. Наибольшие разницы достигают 15%. Анализ, опирающийся на уравнения Навье-Стокса, подтверждает выводы полученные из теории пограничного слоя, которые констатируют, что при установленном $|u_\infty - u_w|$ коэффициент поверхностного трения больше для $u_w > u_\infty$, чем для $u_w < u_\infty$. Разница между значениями уменьшается при убывающих значениях $|u_\infty - u_w|$ и равняется примерно 30% для $|u_\infty - u_w| = 1$ и ниже 1% для $|u_\infty - u_w| = 0{,}1$.

1. Introduction

THE CONCEPT of a continuously moving or pumping plate is illustrated in Fig. 1 which shows a symmetrical arrangement of two belts each running over two pullies. The whole arrangement is situated inside a box the sides of which are two parallel moving regions of the belt which are pumping fluid from the left to the right.

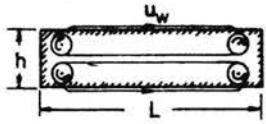

FIG. 1. Pumping plate model.

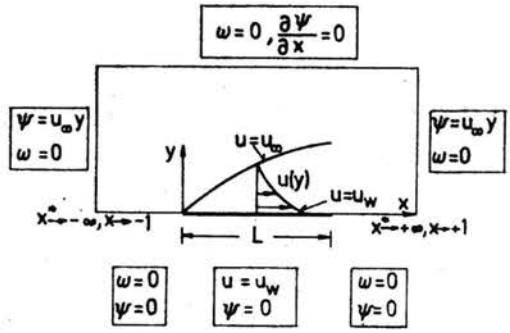

FIG. 2. Flow region and boundary conditions.

In the mathematical model we let the height h tend to zero, see Fig. 2. Thus we obtain a flat plate which is moving while the fluid is initially at rest. Although this problem might look just like the classical Blasius case with the boundary conditions exchanged, there is no Galilean transformation combining the two cases as SAKIADIS [1] first showed. This is due to the plate's special kind of motion. While the two belts of Fig. 1 are running, the whole box does not move in space. Thus the region where the boundary condition of non-zero wall velocity has to be applied is time-independent. In the laboratory system of coordinates we have to solve the steady equation of motion. In a system of coordinates moving with the plate, we had to solve the unsteady equation of motion for the boundary condition of zero wall-velocity.

In the surrounding fluid initially at rest, a boundary layer develops past the pumping plate, the thickness of which is increasing in the same direction as the plate is moving, see Fig. 2. From the boundary layer theory one obtains the result that the skin friction coefficient is about 30% higher than in the BLASIUS case [2].

An infinite plate moving in a cooling bath, a film of condensation running down a wall and a filament extruded from an orifice in the melt spinning process are physical examples where the flow situation presented appears in the field of practical application. From these examples it can be seen that the pumping or continuously moving surface often is accompanied with blowing. Thus the general problem of a pumping plate moving with the velocity u_w in a parallel free stream u_∞ is considered in the present paper.

In the literature for the pumping plate only solutions of the boundary-layer equation are presented. SAKIADIS [1] and SPARROW *et al.* [3] solved the Blasius equation for the pumping plate boundary conditions. In [4, 5] similarity solutions for the pumping plate boundary-layer equation and finite difference solutions for the continuously moving cylinder including the transverse curvature effect were presented.

KLEMP and ACRIVOS [6] considered the problem of uniform flow past a pumping plate whose surface has a constant velocity opposite in direction to that of main-stream for large values of the Reynolds number Re. Basing on the numerical solution of the full Navier-Stokes equations by LEAL and ACRIVOS [7], it was assumed that for $\mathrm{Re} \gg 1$ the region of reverse flow remained within an 0 ($\mathrm{Re}^{-1/2}$) distance from the plate and the problem was dealt with in terms of a moving-wall boundary-layer with a zero pressure gradient. Thus the numerical procedure applied integrated the boundary layer equation.

Several authors investigated the flow field past a flat plate at rest in a uniform free stream by integrating the full Navier-Stokes equations. Our results for this case are compared with those presented by LOER [8] and by FASEL [9]. The results given by DENNIS and DUNWOODY [10] were obtained by first simplifying the Navier-Stokes equations in order to reduce them to ordinary differential equations which afterwards were solved numerically. Their drag coefficient is proportional to $\mathrm{Re}^{-1/2}$ in accordance with the boundary layer theory but the actual calculated value of their coefficient is higher than the Blasius value, whereas the integration of the full Eqs. (3.6) and (3.7) shows the opposite result.

2. Similarity solutions of the boundary layer equation

Introducing the similarity coordinates (overbars represent dimensional quantities)

$$\eta = \bar{y}\sqrt{\frac{\bar{u}_r}{\bar{\nu}\bar{x}}}, \tag{2.1}$$

$$f(\eta) = \frac{\bar{\psi}}{\sqrt{\bar{\nu}\bar{x}\bar{u}_r}}, \tag{2.2}$$

$$u = \bar{u}/\bar{u}_r = f'(\eta), \tag{2.3}$$

$$v = \bar{v}\Big/\left(\frac{1}{2}\sqrt{\bar{\nu}\bar{u}_r/\bar{x}}\right) = \eta f' - f \tag{2.4}$$

with

$$\bar{u}_r = \begin{cases} \bar{u}_\infty & \text{if} \quad \bar{u}_\infty > \bar{u}_w, \\ \bar{u}_w & \text{if} \quad \bar{u}_w > \bar{u}_\infty, \end{cases} \tag{2.5}$$

we obtain the ordinary differential equation first presented by BLASIUS [2]

$$2f''' + ff'' = 0. \tag{2.6}$$

For the pumping plate moving in a fluid initially at rest, the boundary conditions in similarity coordinates are

$$\begin{aligned} &\eta = 0: \quad f' = 1, \quad f = 0, \\ &\eta \to \infty: \quad f' = 0. \end{aligned} \tag{2.7}$$

For this case SAKIADIS [1] obtained the skin friction coefficient (first number in brackets gives the wall velocity, second number gives the velocity at the outer edge of the boundary layer, both in dimensionless coordinates)

$$C_f(1.0; 0.0) = \tau_w/(\bar{\varrho}\bar{u}_w^2) = 0.444/\sqrt{\mathrm{Re}_x} \tag{2.8}$$

with

$$\mathrm{Re}_x = \bar{u}_w \cdot \bar{x}/\bar{\nu}. \tag{2.9}$$

This value is 33% larger than the result presented by Blasius for the classical flow case

$$C_f(0.0; 1.0) = \tau_w/(\bar{\varrho}\bar{u}_\infty^2) = 0.332/\sqrt{\mathrm{Re}_x} \tag{2.10}$$

with

$$\mathrm{Re}_x = \bar{u}_\infty \cdot \bar{x}/\bar{\nu}. \tag{2.11}$$

We now regard the solutions of Eq. (2.6) for cases when the velocity of the plate and the velocity of the fluid are different from zero simultaneously.

Figure 3 shows the skin friction coefficient plotted against the velocity difference between free stream and plate. The velocities are non-dimensionalized according to Eqs. (2.3)

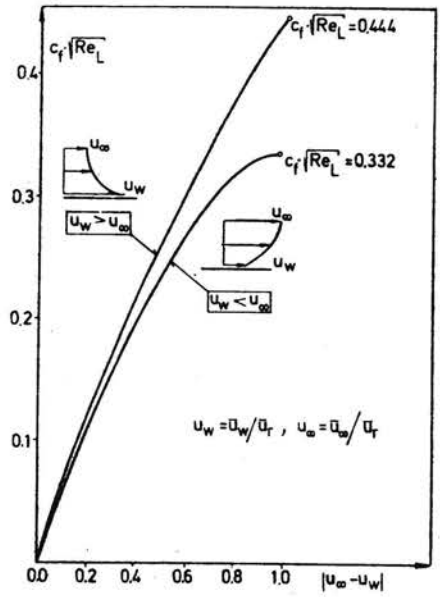

FIG. 3. Skin friction coefficient $c_f\sqrt{\mathrm{Re}_L}$ as function of $|u_\infty - u_w|$. Similarity solutions from the boundary layer theory.
$\bar{u}_r = \bar{u}_\infty$ if $\bar{u}_\infty > \bar{u}_w$, $\bar{u}_r = \bar{u}_w$ if $\bar{u}_\infty < \bar{u}_w$.

and (2.5). The upper curve refers to the case when the plate's velocity is larger than the free stream velocity while the lower curve shows results for the opposite case.

For $|u_\infty - u_w|$ fixed the skin friction coefficient is larger for $u_w > u_\infty$ than for $u_w < u_\infty$. For $|u_\infty - u_w| = 0.8$ e.g. we obtain $c_f\sqrt{\mathrm{Re}_L} = 0.38$ with $u_w/u_\infty = 5.0$ and $c_f\sqrt{\mathrm{Re}_L} = 0.314$ with $u_w/u_\infty = 0.2$. The c_f value for a given Re number not only depends on the velocity difference $|u_\infty - u_w|$ but on the parameter u_w/u_∞, too [4, 5]. The difference between the two c_f values decreases for decreasing values of $|u_\infty - u_w|$ being about 30% for $|u_\infty - u_w| = 1$ and being smaller than 1% for $|u_\infty - u_w| = 0.1$.

In Fig. 4 the forward velocity component u and the normal velocity component v are shown as functions of the similarity coordinate η for four different cases. In each pair of two cases A, B and C, D the velocity differences $|u_\infty - u_w|$ are the same, 1.0 and 0.7, respectively.

Case A represents the classical flat plate problem, case B the pumping plate. The solution of case B is shown in Fig. 4A as a dotted line in such a way that the velocity gradients at the wall for the two cases A and B can be compared. The velocity profile $u = 1 - u$ (1.0, 0.0) is of the same character as that for a flat plate at rest with suction.

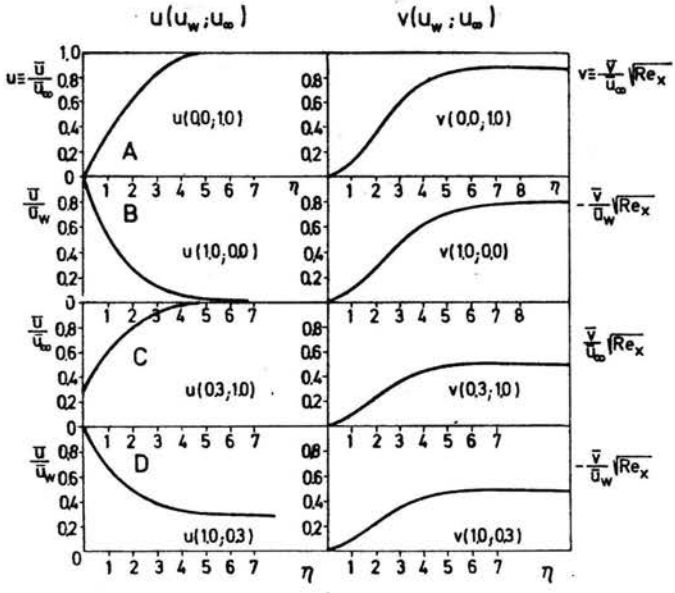

FIG. 4. Velocity profiles. Similarity solutions from the boundary layer theory.
A — Blasius case, B — Sakiadis case.

For the pumping plate, case *B*, the velocity component v is negative, the fluid is sucked towards the plate. In the classical and the pumping plate case the value of the normal velocity component v is zero at the wall and increases with increasing distance from the wall. In the case of a pumping plate the assumption of the boundary layer theory $v \ll u$ is not fulfilled at the outer edge of the boundary layer as there the u-component tends to zero while the v-component remains finite.

In the classical case outside the boundary layer the disturbances resulting from the plate become small as compared with the velocity values of the uniform free stream. Thus the flow field is known there. As in the case of the pumping plate the fluid initially is at rest and even small velocity changes now mean a significant difference as compared to the original situation. Thus the whole flow field is unknown and the outer field can be calculated only by integrating the Navier-Stokes equations numerically.

3. Numerical integration of the Navier-Stokes equation for the pumping plate flow field

Some of the difficulties connected with the numerical solution of the steady Navier-Stokes equations can be avoided if the steady flow is considered as an asymptotic form of a time-dependent flow, thus profiting from the techniques available for the numerical solution of the initial value problems. This is so since the full time-dependent Navier-Stokes equations are parabolic in time. Altough the numerical procedure can imitate the natural development to the final steady flow, in our case this part of the calculation is merely fulfilling the function of an iteration procedure.

Starting from the Navier-Stokes equation written as a vorticity transport equation, one obtains after defining non-dimensionalized quantities

$$x^* = \bar{x}/\bar{L}, \tag{3.1}$$

$$y^* = \bar{y}/\bar{L}, \tag{3.2}$$

$$t = \bar{t}\bar{u}_r/\bar{L}, \tag{3.3}$$

$$u = \bar{u}/\bar{u}_r, \tag{3.4}$$

$$v = \bar{v}/\bar{u}_r \tag{3.5}$$

the equation

$$\frac{\partial\omega}{\partial t} + \frac{\partial}{\partial x^*}(u\omega) + \frac{\partial}{\partial y^*}(v\omega) = \frac{1}{\mathrm{Re}_L}\left(\frac{\partial^2\omega}{\partial x^{*2}} + \frac{\partial^2\omega}{\partial y^{*2}}\right) \tag{3.6}$$

with the vorticity ω and the Reynolds number Re_L

$$\omega = \frac{\partial v}{\partial x^*} - \frac{\partial u}{\partial y^*}, \tag{3.7}$$

$$\mathrm{Re}_L = \bar{u}_r\bar{L}/\bar{\nu}. \tag{3.8}$$

The overbars again represent dimensional quantities. We have $\bar{\nu}$ — kinematic viscosity, $\bar{u}_r$ — reference velocity, see Eq. (2.5). We fulfill the continuity equation identically by introducing the stream function ψ

$$u = \partial\psi/\partial y^*, \tag{3.9}$$

$$v = -\partial\psi/\partial x^*. \tag{3.10}$$

From Eqs. (3.7), (3.9) and (3.10), the Poisson equation for the stream function results:

$$\frac{\partial^2\psi}{\partial x^{*2}} + \frac{\partial^2\psi}{\partial y^{*2}} = -\omega. \tag{3.11}$$

The conditions imposed on the boundaries are

$$\begin{aligned}
&y^* = 0, && -\infty \leqslant x^* < 0: && \omega = 0\ , && \psi = 0,\\
&y^* = 0, && 0 \leqslant x^* \leqslant 1: && u = u_w, && \psi = 0,\\
&y^* = 0, && 1 < x^* \leqslant +\infty: && \omega = 0, && \psi = 0,\\
&0 < y^* \leqslant y^*_{\max}, && x^* \leqslant -\infty: && \omega = 0, && \psi = u_\infty y,\\
&y^* = y^*_{\max}, && -\infty \leqslant x^* \leqslant +\infty: && \omega = 0, && \partial\psi/\partial x = 0,\\
&0 < y^* \leqslant y^*_{\max}, && x^* = +\infty: && \omega = 0, && \psi = u_\infty \cdot y.
\end{aligned} \tag{3.12}$$

We apply the transformation of coordinates given in [1]:

$$\begin{aligned}
x &= \tanh(a_x x^*),\\
y &= \tanh(a_y y^*).
\end{aligned} \tag{3.13}$$

This hyperbolic transformation maps the infinite flow region into a finite one

$$-1 \leqslant x \leqslant 1, \quad 0 \leqslant y \leqslant y_{\max}. \tag{3.14}$$

This makes possible the straifghtforward application of the relevant boundary conditions at very large distances from the plate and at the same time allows to concentrate the grid points of the finite difference scheme near the flat plate where the gradients are large, so that the accuracy in this region is increased.

The upper boundary condition was applied at a finite but sufficiently large distance from the plate, $\bar{y}_{\max} > 10\bar{\delta}_L$, greater than ten times the boundary layer thickness at the trailing edge. The value of a_y is chosen such that the boundary layer is expanded to occupy at least one third of the number of grid points in the y-direction. The origin of coordinates is chosen at the plate's leading edge.

Applying the transformation of Eq. (3.13), we obtain from Eqs. (3.9), (3.10), (3.6) and (3.11)

$$u = F_2(y)\,\partial\psi/\partial y, \tag{3.15}$$

$$v = -F_1(x)\,\partial\psi/\partial x, \tag{3.16}$$

$$\frac{\partial\omega}{\partial t} + F_1(x)\frac{\partial}{\partial x}(u\omega) + F_2(y)\frac{\partial}{\partial y}(v\omega) = \frac{1}{\mathrm{Re}_L}\left[F_3(x)\frac{\partial^2\omega}{\partial x^2} + F_4(y)\frac{\partial^2\omega}{\partial y^2} + F_5(x)\frac{\partial\omega}{\partial x} + F_6(y)\frac{\partial\omega}{\partial y}\right], \tag{3.17}$$

$$F_3(x)\frac{\partial^2\psi}{\partial x^2} + F_4(y)\frac{\partial^2\psi}{\partial y^2} + F_5(x)\frac{\partial\psi}{\partial x} + F_6(y)\frac{\partial\psi}{\partial y} = -\omega \tag{3.18}$$

with

$$\begin{aligned} F_1(x) &= a_x(1-x^2), & F_2(y) &= a_y(1-y^2),\\ F_3(x) &= [F_1(x)]^2, & F_4(y) &= [F_2(y)]^2,\\ F_5(x) &= -2a_x\cdot x\cdot F_1(x), & F_6(y) &= -2a_y\cdot y\cdot F_2(y). \end{aligned} \tag{3.19}$$

The partial differential equations are approximated by an explicit space-centered finite difference scheme, with a fourth-order accurate difference formula for the vorticity generated at the plate surface. The finite approximation of the vorticity transport equation reads, in conservative form (i refers to the x- and j to the y- direction),

$$\begin{aligned} \frac{\omega n_{i,j}-\omega_{i,j}}{\Delta t} = {} & -F_1(i)\frac{(u\omega)_{i+1,j}-(u\omega)_{i-1,j}}{2\Delta x} - F_2(j)\frac{(v\omega)_{i,j+1}-(v\omega)_{i,j-1}}{2\Delta y}\\ & + \frac{1}{\mathrm{Re}_L}\left\{F_3(i)\frac{\omega_{i+1,j}+\omega_{i-1,j}-2\omega_{i,j}}{\Delta x^2} + F_4(j)\frac{\omega_{i,j+1}+\omega_{i,j-1}-2\omega_{i,j}}{\Delta y^2}\right.\\ & \left. + F_5(i)\frac{\omega_{i+1,j}-\omega_{i-1,j}}{2\Delta x} + F_6(j)\frac{\omega_{i,j+1}-\omega_{i,j-1}}{2\Delta y}\right\}. \end{aligned} \tag{3.20}$$

From Eq. (3.20) we obtain the new ω-value which is called $\omega n_{i,j}$. The finite difference approximation of the Poisson equation is

$$\begin{aligned} \omega_{i,j} = {} & F_3(i)[\psi^k_{i+1,j}+\psi n^{k+1}_{i-1,j}-2\psi n^{k+1}_{i,j}]/\Delta x^2 + F_4(j)\,[\psi^k_{i,j+1}+\psi n^{k+1}_{i,j-1}-2\psi n^{k+1}_{i,j}]/\Delta y^2\\ & + F_5(i)\,[\psi^k_{i+1,j}-\psi n^{k+1}_{i-1,j}]/(2\Delta x) + F_6(j)\,[\psi^k_{i,j+1}-\psi n^{k+1}_{j,i-1}]/(2\Delta y). \end{aligned} \tag{3.21}$$

Solving Eq. (3.21) by the Gauss-Seidel procedure with k being the index of iteration, we obtain the new value for the stream function $\psi n_{i,j}$. The velocity components are calculated by means of the following finite difference approximations of Eqs. (3.16), (3.17):

$$u_{i,j} = F_2(j)\,[\psi_{i,j+1} - \psi_{i,j-1}]/(2\Delta y), \tag{3.22}$$

$$v_{i,j} = -F_1(i)\,[\psi_{i+1,j} - \psi_{i-1,j}]/(2\Delta x). \tag{3.23}$$

The number of grid points was 129 in the x-direction and 33 in the y-direction. Thus we had 4257 uniformly-spaced grid points in the field. The a_x- and a_y-values chosen in Eq. (3.13) were $a_x = 0.5$ and $a_y = 2.0, 4.0, 0.62$.

4. Discussion of the results

For all Navier-Stokes results presented in this paper the Reynolds number is $\mathrm{Re}_L = 1000$.

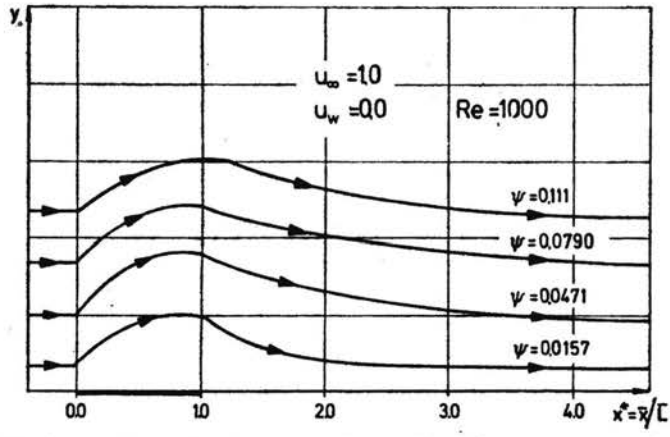

FIG. 5. Field of streamlines. Flat plate at rest in a uniform free stream ($u_w = 0$, $u_\infty = 1.0$).

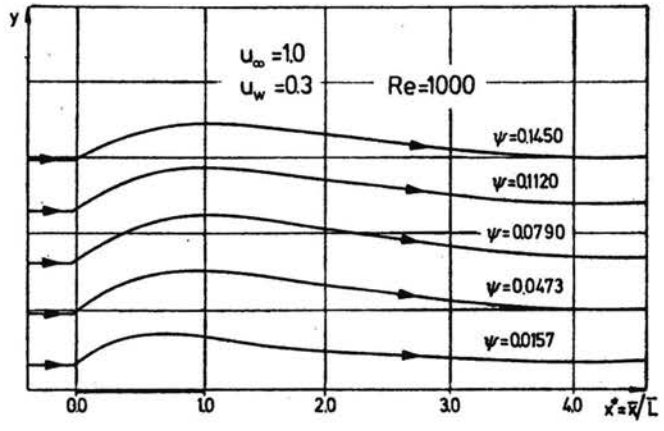

FIG. 6. Field of streamlines. Moving flat plate in a uniform free stream ($u_w = 0.3$ $u_\infty = 1.0$).

In Fig. 5 the field of streamlines is shown for the classical case of a flat plate being at rest in a uniform free stream. The solution is in good agreement with the results shown in the literature [8]. The displacement effect of the plate is demonstrated. There is no strong upstream influence shown by a single plate. The streamlines are deflected away from the plate only a small distance upstream from the leading edge. At about the trailing edge the streamlines start to return gradually to their original y-position which they reach several flat plate lengths downstream.

For a given ψ-value the maximum y-value reached by a streamline is smaller in the case of $u_w = 0.3$ as compared with the case of $u_w = 0$, see Figs. 5 and 6. If the flat plate

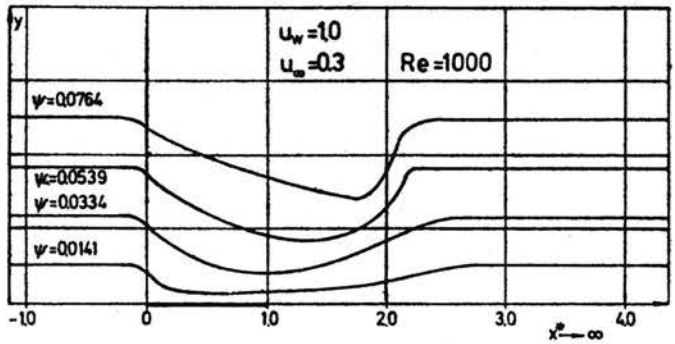

FIG. 7. Field of streamlines. Moving flat plate in a uniform free stream ($u_w = 1.0$, $u_\infty = 0.3$).

is pumping with a velocity smaller than the free stream velocity, the displacement is reduced. But now larger x-values are needed until the streamlines have returned to their original position; there are crossing points between the two systems of streamlines.

When the plate moves faster than the free stream, the pumping effect becomes very obvious, see Fig. 7. Near the leading edge the streamlines are sucked towards the plate, that is the plate receives fluid from the flow field and then pumps it back with an increased velocity as can be seen from the convergence of streamlines. The field of streamlines for the case of a pumping plate moving in a fluid initially at rest shows that all fluid particles

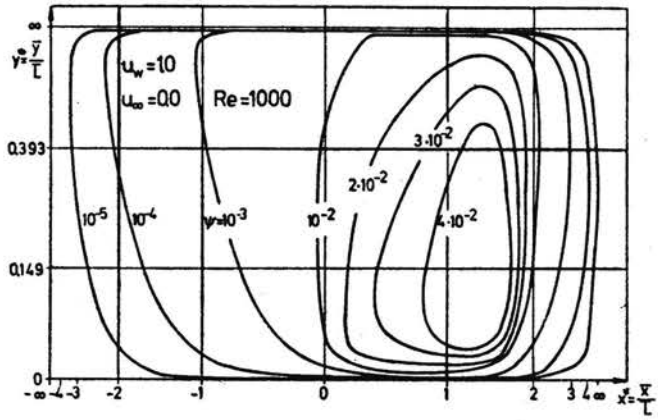

FIG. 8. Pumping plate in a fluid initially at rest ($u_w = 1.0$, $u_\infty = 0.0$).

are set in motion, see Fig. 8. The lowest values of the stream function belong to streamlines near the flat plate. Since the streamlines do not intersect and are closed lines, the fluid particles on these streamlines reach the largest distances from the plate. Along a streamline we have $\psi = \text{const}$. Thus it can be seen from Eq. (3.6) that the velocity of the fluid particles on a given streamline is much larger near the plate than in the region far away from it and approaches zero for $y \to \infty$. Using our Navier-Stokes results we try to answer the question how far the boundary layer theory gives a good approximation for the flow field past a pumping plate. With $v_w = 0$ and $\partial u/\partial x|_w = 0$ we obtain at the wall from the Navier-Stokes equation the relationship

$$\frac{1}{\bar{\varrho}} \frac{\partial \bar{p}}{\partial \bar{x}}\bigg|_w = -\bar{\nu} \frac{\partial \bar{\omega}}{\partial \bar{y}}\bigg|_w . \tag{4.1}$$

According to the first-order boundary layer theory, the forward pressure gradient is zero in the whole flow field in the flat plate case. Then the normal vorticity gradient at the wall is zero, too, and all vorticity necessary to build up the flow field at the plate comes from the leading edge where $\partial^2 u/\partial x^2 \neq 0$ so that $\partial\omega/\partial y \neq 0$. On the basis of the Navier-Stokes equation we cannot assume $\partial p/\partial x|_w = 0$ and we expect normal vorticity gradients different from zero. The vorticity gradient at the wall $\partial\omega/\partial y|_w$ shows whether the assumptions of the boundary layer theory are fulfilled.

In Fig. 9 vorticity profiles obtained by numerical integration of the Navier-Stokes equation are shown. Near the leading edge values for $\partial\omega/\partial y|_w$ are rather large. Only

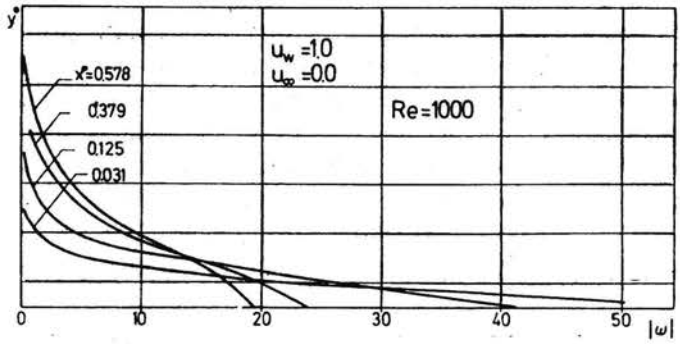

Fig. 9. Vorticity profiles. Pumping plate in a fluid initially at rest ($u_w = 1.0$, $u_\infty = 0.0$).

about one third of the plate length away from the leading edge the normal vorticity gradient at the plate becomes zero approximately. Therefore, especially near the leading edge we expect larger differences between boundary layer and Navier-Stokes results.

This is confirmed by Fig. 10 showing the local skin friction coefficient along the flat plate for cases when the plate moves faster than the fluid obtained by the Navier-Stokes and boundary layer theory. The local skin friction coefficient calculated from the Navier-Stokes solution, is higher than that calculated from the boundary layer theory, the largest differences being of about 15%. These differences are of the same order of magnitude as those obtained for the classical case, see [8, 9]. But in the classical case the Navier-Stokes solutions are smaller. This result should be related to the fact that the boundary layer theory neglects pressure gradients normal to the wall and that the moving plate

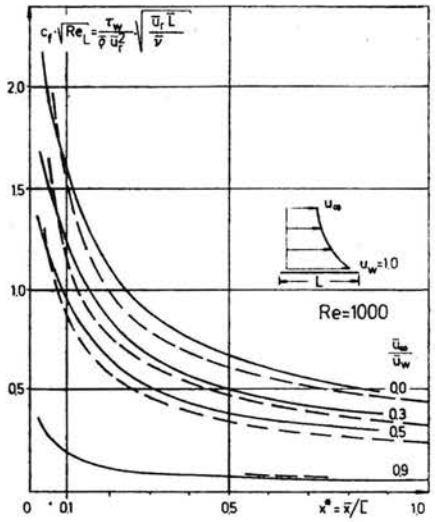

FIG. 10. Pumping plate skin friction coefficient. Navier-Stokes solutions compared with the boundary layer theory.
— — — Boundary layer theory, ——— Navier-Stokes solutions.

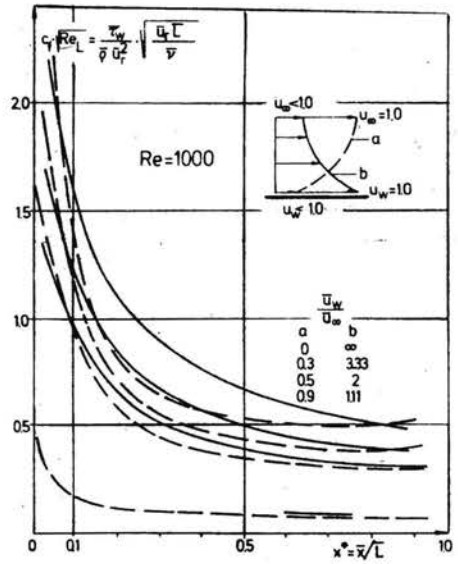

FIG. 11. Pumping plate skin friction coefficient as function of the parameter u_w/u_∞, Navier-Stokes solutions.

is sucking fluid from the flow field towards the plate, while in the classical case fluid is pushed away from the plate.

The Navier-Stokes solutions qualitatively confirm the results obtained from the boundary layer theory which show that for the velocity differences between plate and free stream being constant, higher velocity values of the plate, that is higher values of the parameter $\bar{u}_w/\bar{u}_\infty$, give higher values of the friction coefficient, see Fig. 11.

References

1. B. C. SKIADIS, *Boundary-layer behaviour on continuous solid surface*, A.I.Ch.E. Journ., **7**, 1, 26–28, 1961; **7**, 2, 221–225, 1961.
2. H. BLASIUS, *Grenzschichten in Flüssigkeiten mit kleiner Reibung*, 2, Math Phys., **56**, 1–37, 1908.
3. F. K. TSOU, E. M. SPARROW and R. J. GOLDSTEIN, *Flow and heat transfer in the boundary layer on a continuous moving surface*, Int. J. Heat Mass Transfer, **10**, 219–235, 1967.
4. B. GAMPERT, *Grenzschichttheoretische Probleme des aerodynamischen Schmelzspinnprozesses*, Dissertation Technische Universität Berlin, Berlin 1973.
5. B. GAMPERT, *Die Auslegung von Überschallblasdüsen beim aerodynamischen Schmelzspinnprozess*, VDI-Berichte 290, 253–260, 1977, Chemie-Ingenieur-Technik, **49**, 4, 361, 1977.
6. J. B. KLEMP and A. ACRIVOS, *A moving-wall boundary layer with reverse flow*, J. Fluid Mech., **76**, part 2, 363–381, 1976.
7. L. G. LEAL and A. ACRIVOS, *Structure of steady closed streamline flows within a boundary layer*, Phys. Fluids Suppl., 2, 105, 1969.
8. S. LOER, *Eine numerische Methode zur Lösung der Navier-Stokesschen Gleichungen für zweidimensionale, inkompressible stationäre Strömung längs einer dünnen Platte*, Ingenieur-Arch., 41, 28–39, 1971.

9. H. FASEL, *Numerische Integration der Navier-Stokes-Gleichungen für die zweidimensionale, inkompressible Strömung längs einer ebenen Platte*, ZAMM, **53**, 236–238, 1973.
10. S. C. R. DENNIS and J. DUNWOODY, *The steady flow of a viscous fluid past a flat plate*, J. Fluid Mech., **24**, 3, 577–595, 1966.
11. S. A. SHILLS, *Transformations for infinite regions and their application to flow problems*, AIAA Journ., **7**, 1, 117–123, 1969.

UNIVERSITÄT ESSEN, GESAMTHOCHSCHULE,
FACHGEBIET STRÖMUNGSLEHRE, ESSEN, FRG.

Received October 25, 1979.